Lattice-Dynamical Study of the 110°K Phase Transition in $SrTiO_3$†

G. SHIRANE AND Y. YAMADA*
Brookhaven National Laboratory, Upton, New York 11973
(Received 15 August 1968)

The lattice-dynamical characteristic of the 110°K transition in $SrTiO_3$ has been elucidated by inelastic neutron scattering measurements. The transition is caused by a Γ_{25} soft-phonon mode at the [111] zone boundary, confirming the model recently proposed by Fleury, Scott, and Worlock. The square of the frequency of this soft mode is proportional to $T-T_0$ above the transition temperature T_0. At the transition, this zone boundary becomes a superlattice point, enlarging the unit cell. The results of elastic intensity measurements at the superlattice points at 78°K are consistent with the structure given by Unoki and Sakudo in its space group $I4/mcm$ (D_{4h}^{18}) as well as in the oxygen parameter. This structure is shown to be a logical consequence of the condensed soft mode.

I. INTRODUCTION

In recent years, $SrTiO_3$ has been a subject of extensive studies mainly because of its ferroelectric properties with an expected Curie temperature around 0°K. It is now well established[1–4] that the soft optical mode at $q=0$ is responsible for its high dielectric constant. In addition, $SrTiO_3$ is known to undergo a phase transition at 110°K, which shows extremely interesting characteristics. This transition is *not* accompanied by any anomalies in the dielectric constant.[5] Thus no anomaly was observed in $q=0$ phonons through this transition.[3,4,6] The x-ray study by Lytle[7] revealed a small tetragonal distortion $c/a=1.0005$ below 110°K but the unit-cell volume remains unchanged through the transition. This small tetragonal distortion manifests itself in the ESR experiments.[8] The most remarkable change at the transition was revealed, however, by the elastic-constant measurements.[5]

An attractive feature of this transition lies in its extremely small lattice distortion, indicative of a second-order phase change, combined with other well-defined anomalies. In addition, the crystal structure is a simple perovskite and a large single crystal is readily available.

Cowley[3] proposed a mechanism of this transition based on an accidental degeneracy of the frequencies of two phonon branches in a wide q range. No conclusive experimental verification has since been given for this model. Recently, Unoki and Sakudo[9] suggested an entirely different mechanism in their paper on ESR measurements. They deduced the crystal structure of the low-temperature phase from the atomic positions of oxygen ions as shown in Fig. 1. This structure has a unit cell of $\sqrt{2}a\times\sqrt{2}a\times 2c$ and has a space group $I4/mcm$ (D_{4h}^{18}). Here a and c correspond to the tetragonal one-molecule unit. Unoki and Sakudo then stated that this structure "seems to suggest the occurrence of the instability in some optical branch at large wave vector."

This suggestion was made into a concrete model by Fleury *et al.*[10] in their recent study of $SrTiO_3$. They interpreted their Raman spectrum *below* 110°K based upon the model that the Γ_{25} phonon at the R point, namely, the [111] zone boundary, softens as the temperature decreases to 110°K. This specific model corresponds to a logical conclusion if one believes that the Unoki-Sakudo structure is the consequence of the soft-mode instability.

The present paper reports inelastic neutron scattering experiments which prove conclusively that the 110°K transition is indeed caused by a soft-mode instability at the [111] zone boundary. In addition, the neutron intensity distribution in the low-temperature phase is in essential agreement with the Raman measurements by Fleury *et al.*[10] and the crystal structure deduced by Unoki and Sakudo.[9]

II. EXPERIMENTAL

Two single crystals of $SrTiO_3$ used in the present experiments were obtained from the National Lead Company. They have cylindrical shape of approxi-

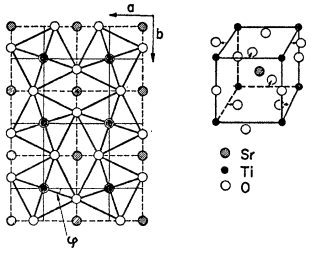

FIG. 1. Oxygen positions in the tetragonal ab plane deduced by Unoki and Sakudo. (Ref. 9).

† Work performed under the auspices of the U. S. Atomic Energy Commission.
* Present address: Osaka University, Osaka, Japan.
[1] W. Cochran, Advan. Phys. **9**, 387 (1960).
[2] P. W. Anderson, in *Fizika Dielectrikov*, edited by G. I. Skanavi (Academcy of Sciences of the USSR, Moscow, 1960).
[3] R. A. Cowley, Phys. Rev. **134**, A981 (1964).
[4] J. M. Worlock and P. A. Fleury, Phys. Rev. Letters **19**, 1176 (1967).
[5] R. O. Bell and G. Rupprecht, Phys. Rev. **129**, 90 (1963).
[6] Y. Yamada and G. Shirane, J. Phys. Soc. Japan (to be published).
[7] F. W. Lytle, J. Appl. Phys. **35**, 2212 (1964).
[8] L. Rimai and G. de Mars, Phys. Rev. **127**, 702 (1962).
[9] H. Unoki and T. Sakudo, J. Phys. Soc. Japan **23**, 546 (1967).
[10] P. A. Fleury, J. F. Scott, and J. M. Worlock, Phys. Rev. Letters **21**, 16 (1968).

mately 0.7 in. in diam and 1.5 in. in height, with the cylinder axis nearly parallel to the [001] or [110]. Their mosaic spread is approximately 0.15°. These are the identical crystals used in our recent measurements on the $q=0$ soft mode.[6]

Inelastic neutron measurements were carried out on a triple-axis spectrometer at the high-flux beam reactor. The constant-Q technique was utilized, with either the incoming neutron energy E_0 or the final energy E_f fixed. These neutron energies were varied between 10 and 50 meV, depending upon the desired instrumental resolution. The effective collimation of neutron beam was 20′ before and after the scattering.

The temperature of the crystals was regulated to within $\pm 0.1°$.

III. PHONON DISPERSION RELATION AT 120°K

A systematic investigation of phonon spectrum at 120°K, just above the transition, has been carried out in search of a soft mode or critical scattering (overdamped mode) associated with the 110°K transition. The effort was centered on the phonons near the zone center as well as the zone boundaries of high-symmetry directions. During this search, as yet unsuccessful, the R-point model by Fleury *et al.*[10] was brought to our attention.

Our recent study[6] revealed no anomaly of the $q=0$ ferroelectric mode in frequency, intensity, and linewidth through the 110°K transition. The same conclusion was reached for several transverse acoustic modes with $q=0.1$–0.2 Å^{-1}. No evidence was found for critical scattering with small q values. Critical scattering, if found, could have been interpreted as an overdamped phonon mode or a tunneling mode.

There are four zone-boundary phonons of interest with high symmetry: one each along the [100] and [111] directions and two along the [110] direction. The last two are characterized by the polarization vector ξ along [001] or [1$\bar{1}$0]. The [100] zone-boundary phonon was reported by Cowley[3] to be temperature-independent. Our brief survey of [110] zone boundary with ξ along [001] revealed that the lowest excitation at 120°K is 13 meV. The other [110] branch with ξ along [1$\bar{1}$0] revealed an interesting feature, which is illustrated in Fig. 2. Not only is it a rather soft mode, with an energy of 8 meV, but it also has a steep negative slope for wave vector approaching the zone boundary. However, the lowest zone-boundary phonon M_3 was shown to be temperature-independent between 120 and 90°K.

Figure 3 shows the transverse [111] branches at 120°K, and representative phonon groups are illustrated in Fig. 4. There are amazing similarities between the two sets of dispersion curves in Figs. 2 and 3. The lowest mode at the [111] zone boundary, however, *is* temperature-dependent, as will be described in Sec. IV. This mode at the R point (the [111] zone

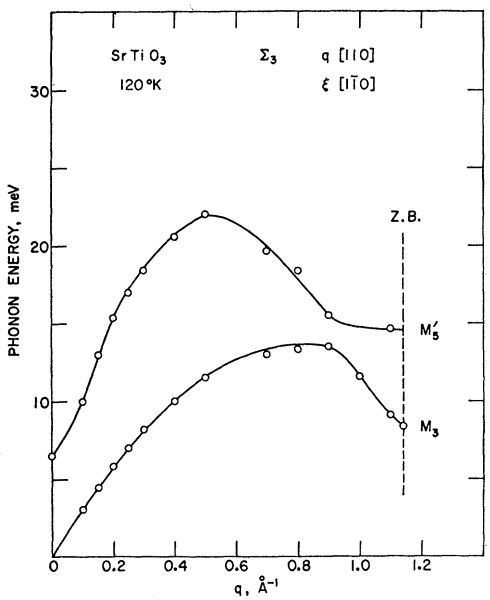

FIG. 2. Two lowest transverse branches with $\mathbf{q}\|[110]$ and $\xi\|[1\bar{1}0]$. The zone boundary corresponds to $q=1.140$ Å^{-1}. The irreducible representations $M3$ and $M5'$ were assigned by Cowley (Ref. 3).

boundary) was assigned as Γ_{25} by Cowley in his calculated dispersion curves (Fig. 10 of Ref. 3). Note that the observed dispersion curves in both [110] and [111] directions are in over-all agreement with Cowley's calculations. It is significant that the calculations by Cowley were based on the observed dispersion curves of the [100] direction alone and they indicated the Γ_{25} mode to be temperature-dependent.

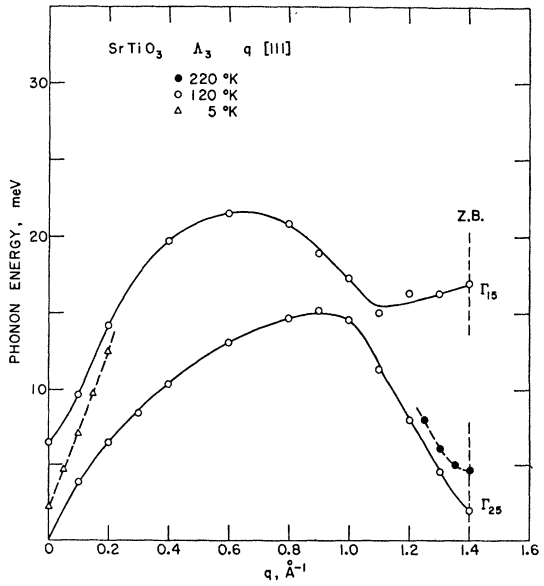

FIG. 3. The lowest transverse branches with $\mathbf{q}\|[111]$. The zone boundary corresponds to $q=1.396$ Å^{-1} at 120°K. Conversion factor from meV to the optical wave number (cm^{-1}) is 8.07.

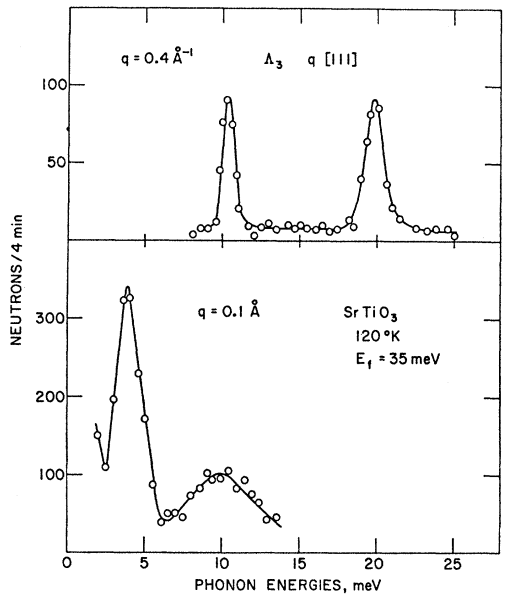

FIG. 4. Phonon groups observed at 120°K. The profiles are mainly determined by the instrumental resolution functions as explained in the text.

IV. 110°K TRANSITION

The Γ_{25} phonon was investigated as a function of temperature through the 110°K transition. As shown in Figs. 5 and 6, the frequency of this mode approaches zero as the temperature is lowered to the transition region. The center peak in Fig. 6 at $\Delta E=0$ corresponds to the incoherent scattering of Sr and Ti as well as small higher-order contaminations, λ/n. The phonon is well defined down to 112°K. Below this temperature and the extrapolated transition temperature $T_0=108$°K the Γ_{25} phonon was not clearly resolved, appearing as a shoulder on the side of the incoherent cross section. The upper limit of the region where the phonon is critically overdamped is $T-T_0=4$°K.

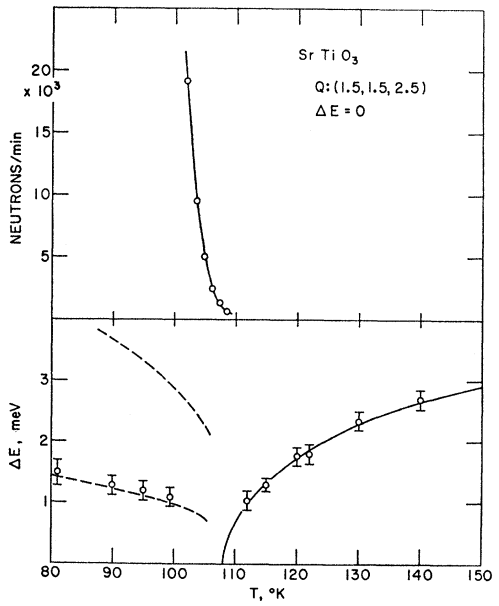

FIG. 5. Temperature dependence of the Γ_{25} mode at the R point. The top figure represents the Bragg intensities at the R point which becomes $q=0$ of the enlarged cell below the transition.

The observed line profiles shown in Fig. 6, as well as in the other figures, are mainly determined by the instrumental resolution function, in $E-q$ space, in relation to the dispersion surface under investigation.[11] No special effort was made, in the present investigation, to extract accurate phonon lifetimes. However, a rough estimate sets an upper limit of the intrinsic linewidth (full width at half-maximum) of 0.6 meV at 112°K.

The reciprocal of the square of Γ_{25} phonon energies follow approximately a Curie-Weiss law. However, the high-temperature data shown in Fig. 7 clearly demand a temperature-independent term. Thus a satisfactory fit is attained by

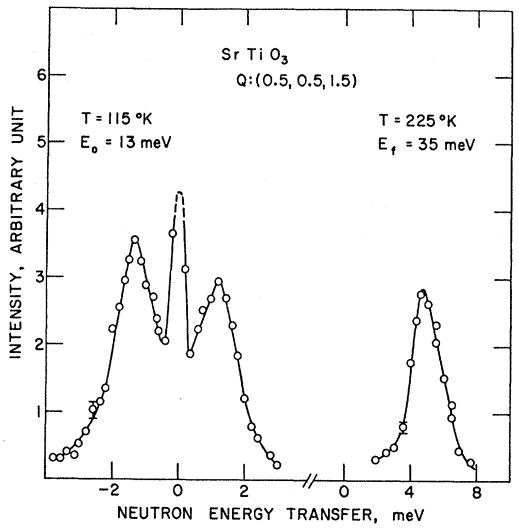

FIG. 6. Profiles of the Γ_{25} mode above the transition. Positive sign in the energy axis corresponds to neutron energy loss.

$$1/\hbar^2\omega^2=a+c/(T-T_0), \qquad (1)$$

with

$$T_0=108\text{°K}, \quad a=0.0081\ \text{meV}^{-2}, \quad c=4.22\ \text{meV}^{-2}\,\text{deg}.$$

The solid lines in Figs. 5 and 7 represent Eq. (1) with the parameters given above. The constant term a gives a "saturation" energy of 11 meV at the high-temperature limit. A similar constant term for the $q=0$ ferroelectric mode was emphasized by Rupprecht and Bell[12] in their dielectric measurements.

At the transition point, defined as T_0 in Eq. (1), the R point becomes new Bragg position which enlarges the

[11] M. J. Cooper and R. Nathans, Acta Cryst. 23, 357 (1967).
[12] G. Rupprecht and R. O. Bell, Phys. Rev. 135, A748 (1964).

cubic cell. We shall call these new reflections "superlattice points," and index them with half-integers. The intensity of the $\frac{1}{2}(533)$ reflection near the transition temperature is shown in Fig. 5. Because of the large size of the crystals, a probable extinction effect makes the relative intensities unreliable. Nevertheless, the basic feature of a second-order transition is well illustrated.

Below the transition temperature the crystal symmetry becomes tetragonal, as has been established by x-ray[7] and ESR measurements.[8,9] The crystal then consists of three types of domains with different c directions. The original Γ_{25} mode, which is triply degenerate in the cubic phase, is now split into two modes depending upon whether the polarization vector ξ is perpendicular to

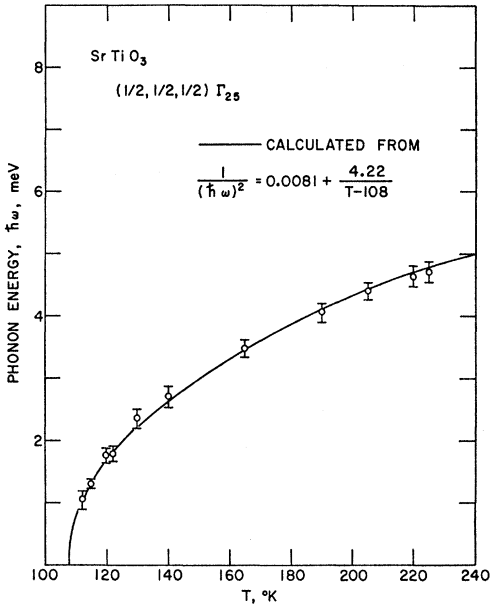

FIG. 7. Temperature dependence of the Γ_{25} mode above the transition. Solid line represents a modified Curie-Weiss law as explained in the text.

(doublet) or parallel to (singlet) the c axis. These are the two observed Raman lines indentified as E_g and A_{1g} by Fleury *et al.*[10] (In this notation Γ_{25} should be called F_{2u}.) These two lines were also called A and D, respectively, in the early paper by Worlock and Fleury.[4] We adopt the notation A and D for convenience.

The A line was easily observed as is shown in Fig. 5. This phonon could not be clearly resolved between 100 and 108°K. A part of the low-energy background, which masks this soft mode, is now contributed by low-energy acoustic phonons, since the cubic R point becomes the zone center in the tetragonal phase. The D line is considerably weaker in intensity, as shown in Fig. 8. The intensity in D, when compared with A, is consistent with its higher energy and its singlet character. As

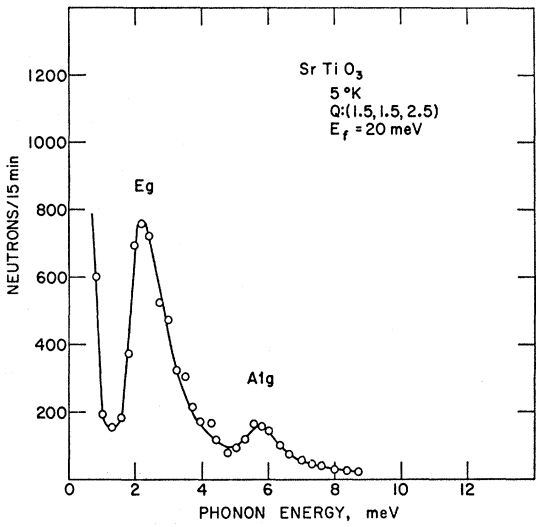

FIG. 8. Profiles of the two lowest phonons at the original R point, which becomes the zone center below 110°K. The assignment of lines, E_g (A line) and A_{1g} (D line), are due to Fleury *et al.* (Ref. 10).

shown in Fig. 9, the neutron data are in excellent agreement with the Raman results. The latter are represented by smoothed solid lines for the measured region and by broken lines for the extrapolated region.

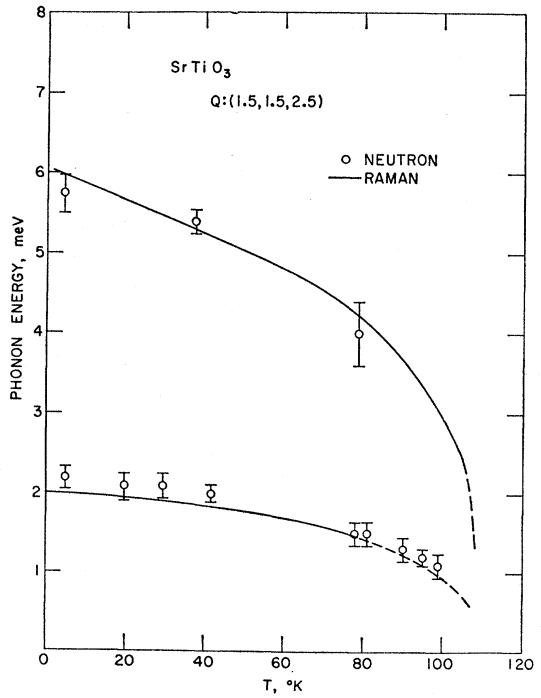

FIG. 9. Temperature dependence of A and D lines in the tetragonal phase. The solid lines correspond to observed Raman data and dotted lines correspond to extrapolated Raman data by Fleury *et al.* (Ref. 10).

V. CRYSTAL STRUCTURE AT 78°K

A limited effort was made to determine the crystal structure of the low-temperature phase by studying the elastic scattering from several reciprocal lattice points. The large size of the crystals requires a formidable extinction correction for the strong reflections and double-Bragg correction for the weaker reflections. Moreover, domain formation in the tetragonal phase does not permit a unique indexing of the reflections, since the angular resolution of the neutron spectrometer is not sufficient to resolve the split peaks because of the small c/a ratio of 1.0006. We make the following assumptions: (a) The symmetry of the crystal structure is tetragonal, and (b) the domains are randomly distributed among the three c directions. Then we compare the observed intensity distribution with the structure proposed by Unoki and Sakudo. Their structural parameters are given in Table I and illustrated in Fig. 1.

The permitted reflections in this group, $I4/mcm$, are given in terms of true tetragonal indexing (unit cell $\sqrt{2}a\times\sqrt{2}a\times 2c$ and suffixed):

$$\begin{aligned} &h_t k_t l_t, \quad h_t+k_t+l_t=2n; \\ &h_t 0 l_t, \qquad h_t(l_t)=2n. \end{aligned} \tag{2}$$

When converted to a pseudocubic indexing scheme with random domains, the first condition gives that all the new reflections should have half-integers in all h, k, and l. This is confirmed in the intensity study of the two projections $(h0l)$ and (hhl); namely, the only new reflections observed were limited to those with h and l half-integers in the second projection. The $\frac{1}{2}(hhh)$ should, however, be missing because of the second condition given above. The intensity data obtained at 1.1 Å gave weak but observable intensities at $\frac{1}{2}(111)$ and $\frac{1}{2}(333)$. A systematic investigation of the intensity ratio between $\frac{1}{2}(111)$ and $\frac{1}{2}(113)$ was carried out as a function of wavelength up to 2.5 Å. The observed intensity of $\frac{1}{2}(111)$ at lower wavelength was shown to be mainly double-Bragg scattering.[13] Thus the observed superstructure lines are in agreement with the space group $I4/mcm$.

The structure factor of the superlattice lines involves only the oxygen atoms with the positional parameter x.

TABLE I. Structural parameters of $SrTiO_3$ at 78°K given by Unoki and Sakudo; a and c correspond to the tetragonal cell containing one molecular unit ($z=1$).

Space group Unit cell	$D_{4h}^{18}(I4/mcm)$ $\sqrt{2}a\times\sqrt{2}a\times 2c$	($z=4$)	
4 Ti	000	$00\frac{1}{2}$	$(+\frac{1}{2}\frac{1}{2}\frac{1}{2})$
4 Sr	$0\frac{1}{2}\frac{1}{4}$	$\frac{1}{2}0\frac{1}{4}$	
4 O	$00\frac{1}{4}$	$00\frac{3}{4}$	
8 O	$\pm(x,\frac{1}{2}+x,0)$	$\pm(\frac{1}{2}+x,\bar{x},0)$	
	$x=0.244$		

This can be written as a deviation from the cubic position:

$$x=0.25-\delta=0.25-\tfrac{1}{4}\sin\varphi, \tag{3}$$

where φ is the rotation parameter given by Unoki and Sakudo (see Fig. 1). The value of φ at 78°K was given as 1.4°, which gives $\delta=0.006$. The structure factor is now given as

$$F\propto 8\sin 2\pi h_t\delta\cong 16\pi h_t\delta. \tag{4}$$

Here we selected axes to make h_t even and k_t odd.

The intensity data obtained at $\lambda=1.1$ Å are compared with the calculated ones in Table II. The superlattice reflections can be grouped by the value of h_t, as expected. The accuracy of the observed data for the first and the last groups in the table is least reliable, probably not better than 30%, because of the double-Bragg and extinction effects, respectively. Over-all agreement is satisfactory. Moreover, the sensitivity of the intensities on δ^2 permit us to determine the parameter x quite accurately with the available data alone:

$$x=0.244\pm 0.0015.$$

This is exactly the value given by Unoki and Sadudo at 78°K.

TABLE II. Intensity comparison of $SrTiO_3$ at 78°K. The calculated values correspond to $x=0.244$, random domain, and the scattering length of Sr (0.66), Ti (−0.33), and O (0.58). The temperature factor is neglected. Upper limit of the unobserved intensity is less than 2 in the unit of this table.

$(hhl)\times 2$	$h_t k_t l_t$	I_{calc}	I_{obs}
113, 115, 331 337, 551, 773	211, 231, 213 253, 235, 257	15	13–25
117, 119, 335 355, 177	431, 451, 413 415, 437	56–60	45–70
339, 557, 775	633, 615, 617	130–136	100–110
022, 422, 822 066, 466	200, 112, etc.	170–190	150–200
600, 442, 446	006, 330, etc.	490–570	450–630

VI. DISCUSSION

We have just presented conclusive experimental evidence that the 110°K transition in $SrTiO_3$ is caused by a condensation of the Γ_{25} mode at the [111] zone boundary. We have also shown that the space group of the low-temperature phase is $I4/mcm$. Now let us examine the relation between the vibrational displacement of oxygen in the cubic phase and the condensed structure below 110°K. A general problem of this nature has been treated theoretically by several authors[14–16] and recently discussed by Cochran and Zia[17] in connection with several perovskite-type antiferroelectrics. In

[13] At present we cannot exclude the possibility that weak $\frac{1}{2}(hhh)$-type lines exist. If these are genuine, the probable tetragonal space group is $I4/m$.

[14] P. C. Kwok and P. B. Miller, Phys. Rev. **151**, 387 (1966); P. B. Miller and P. C. Kwok, Solid State Commun. **5**, 57 (1967).
[15] R. A. Cowley, Phil. Mag. **11**, 673 (1965).
[16] C. Haas, Phys. Rev. **140**, A863 (1965).
[17] W. Cochran and A. Zia, Phys. Status Solidi **25**, 273 (1968).

particular, the discussion of a transition in $LaAlO_3$ by Cochran and Zia[17] has an interesting bearing on the present subject.

The atomic displacements of Γ_{25} $(\frac{1}{2}\frac{1}{2}\frac{1}{2})$ involves only the oxygen atoms[3] as shown in Fig. 10 and Table III. This mode is triply degenerate, which is illustrated by the A, B, and C atomic motions (unit vector) in Table III. If mode A condenses at the transition point, the resulting structure has the tetragonal symmetry $I4/mcm$. On the other hand, $A+B+C$ give a rhombohedral structure, $R\bar{3}C$. The last case was the model proposed by Cochran and Zia for $LaAlO_3$. The discussion presented above is very closely related to three stable phases of $BaTiO_3$, i.e., the polarization is either the [100], [110], or [111] direction.

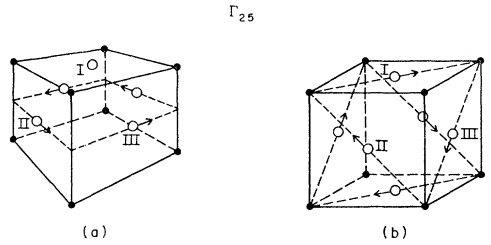

FIG. 10. Displacement of oxygens in the Γ_{25} mode. (a) Corresponds to $O_{IIx}=-O_{IIIy}$ and (b) corresponds to a linear combination of these ($A+B+C$ in Table III).

The inelastic structure factor for the A mode in the cubic phase can be given as

$$F_{\text{inel}} \propto \sum_j (\mathbf{Q}\cdot\xi_j) e^{i\mathbf{Q}\cdot\mathbf{r}_j}, \tag{5}$$

where

$$\mathbf{Q}=2\pi\boldsymbol{\tau}+\mathbf{q}(\tfrac{1}{2}\tfrac{1}{2}\tfrac{1}{2}).$$

This $\mathbf{Q}$ can be given as (hkl) all half-integers. If we choose the axis to make $h+k=2n$ and $h-k=2n+1$, then

$$F_{\text{inel}} \propto (h+k)=h_t. \tag{6}$$

The intensities of inelastic scattering are contributed equally by this A mode as well as B and C modes. A comparison of Eqs. (6) and (4) shows that the Bragg intensities at the superlattice points in the tetragonal phase, with random domains, are identical to those of the corresponding inelastic scattering in the cubic phase, except for a scale factor. Experimentally, no quantitative measurements were done on the absolute intensities of the Γ_{25} phonons at different zone boundaries. However, the phonon intensities at the three points $\frac{1}{2}(113)$, $\frac{1}{2}(333)$, and $\frac{1}{2}(335)$ are in qualitative agreement with the condensed Bragg intensities below the transition; in particular, the phonon at $\frac{1}{2}(333)$ is extremely weak, if it exists at all.

It may be interesting to note an uncertainty of the structure determination in the condensed phase when the soft mode is degenerate. This occurs, as often is the case, when (a) the condensed phase has a random domain distribution, (b) the lattice distortion is too small to permit a separation of the once-equivalent reflections, and (c) the atomic shift δ is small so that $\sin 2\pi h\delta \cong 2\pi h\delta$. The number of structures generated by linear combinations of the degenerate modes give almost identical intensity distributions. For example, in the present case of the Γ_{25} at $(\frac{1}{2}\frac{1}{2}\frac{1}{2})$, the $R\bar{3}C$ structure, which corresponds to $A+B+C$ [Fig. 10(b)], as well as an orthorhombic structure $(A+B)$, cannot be easily distinguished from the tetragonal $I4/mcm$ from the intensity data alone.

TABLE III. Polarization vectors ξ of the Γ_{25} mode at $(\frac{1}{2}\frac{1}{2}\frac{1}{2})$.

Oxygen	$\mathbf{r}_j$	$\xi_j(A)$	$\xi_j(A+B+C)$
I	$(\frac{1}{2}\frac{1}{2}0)$	(0 0 0)	(1 1 0)
II	$(\frac{1}{2}0\frac{1}{2})$	(1 0 0)	(1 0 −1)
III	$(0\frac{1}{2}\frac{1}{2})$	(0 −1 0)	(0 −1 −1)
A	$O_{IIx}=-O_{IIIy}$		
B	$O_{Ix}=-O_{IIIz}$		
C	$O_{Iy}=-O_{IIz}$		

A similar uncertainty has been known for magnetic-structure determination of a pseudocubic crystal such as MnO and Cr. One can remove the degeneracy by unbalancing the domains either by an uniaxial stress or by simply making a crystal more perfect. In the present case, the tetragonal symmetry of $SrTiO_3$ appears to have been well established.[7–9]

We have developed a logical relation between the soft mode above the 110°K transition in $SrTiO_3$ and the structure of the condensed phase. This is indeed a simple and elegant mechanism by which the transition can take place, just as the case of the $q=0$ ferroelectric soft mode.[1,2] It is also quite likely that this is the mechanism of many other transitions in perovskite-type crystals. What makes the 110°K transition in $SrTiO_3$ particularly attractive for a lattice-dynamical study is the fact that the soft phonon remains well defined even when it reaches a very low frequency near the transition. Phenomenologically, the observed Curie-Weiss law corresponds to the leading term of the free-energy expansion in terms of lattice-dynamical parameters.[14–17] One of the remaining problems is a theoretical study of the relative stability of $I4/mcm$ and $R\bar{3}C$ in terms of anharmonic interactions. Experimentally, a detailed investigation of phonon lifetime near the transition may reveal interesting information concerning the anharmonicity of the soft mode.

ACKNOWLEDGMENTS

We are very grateful to J. D. Axe, M. Blume, V. J. Minkiewicz, and J. M. Worlock for illuminating discussions and to P. A. Fleury, J. F. Scott, and J. M. Worlock for giving us an opportunity to study their paper prior to publication.